The internal strain parameter of diamond from synchrotron radiation measurements

The internal strain parameter of diamond from synchrotron radiation measurements

C S G Cousins†, L Gerward‡§, J Staun Olsen‖ and B J Sheldon†

† Physics Department, Exeter University, Exeter, Devon, UK
‡ Laboratory of Applied Physics, Bldg. 307, Technical University of Denmark, DK-2800 Lyngby, Denmark
‖ Physics Laboratory H C Ørsted Institute, Copenhagen, Denmark

Abstract. The internal strain parameter of diamond has been found from the uniaxial stress-dependence of the integrated intensity of the 'forbidden' 006 reflection. Synchrotron radiation from the storage ring DORIS–HASYLAB was conditioned by a gold mirror to provide the 006 and 008 reflections from the sample. Integrated intensities were recorded using an energy-dispersive method. The value found is $\bar{A} = -0.031 \pm 0.005$ and corresponds to a bond-bending parameter $\zeta = 0.125 \pm 0.020$. This value is in accord with two recent theoretical values based on a bond-charge model and on an *ab initio* pseudopotential calculation.

1. Introduction

We have previously measured (Cousins *et al* 1982a, 1982b) and remeasured (Cousins *et al* 1987) the internal strain parameters of silicon and germanium using the energy-dispersive x-ray diffraction technique. This type of measurement, using bremsstrahlung from an x-ray tube, is applicable to relatively few materials because it requires the study of the stress-dependence of a reflection that is either strictly forbidden or very weak in the absence of stress: Si and Ge come in the former category, GaAs and InSb in the latter. Other materials require inordinately long measurement times.

The natural progression of our studies towards diamond itself was hindered by two factors: firstly the scattering power of carbon is small and secondly the internal strain parameter is predicted to be as much as a factor of six smaller than that of Si or Ge (Nielsen 1986). Both these problems are overcome by the use of synchrotron radiation. Not only is the intensity greater but a novel experimental procedure may be used to optimise the measurements. The latter exploits the use of a totally reflecting gold mirror to reduce the intensity of the strong high-order reflections that would otherwise saturate the detector.

The reason for our remeasurement of Si and Ge was a suspicion, subsequently confirmed, that the strain in the surface of the crystals was not the same as the mean strain deduced from elasticity theory. The cause of this discrepancy is believed to be elastic mismatch between the anvils of the uniaxial press and the sample. In the present

§ Author to whom all correspondence should be addressed.

work this problem is solved by taking measurements in transmission, thereby sampling the mean strain rather than the surface strain.

In § 2 we recall the theory behind the measurement, in § 3 we describe the way it is achieved in practice and in § 4 and § 5 we present results and conclusions.

2. Résumé of theory

The internal strain formalism for the diamond structure is set out in Cousins *et al* (1982a). The following is a summary of the part relevant to diffraction.

The square of the structure factor of an unstressed diamond crystal is

$$|F_H|_0^2 = 32f_H^2(1 + \cos \varphi_H) \tag{1}$$

where the phase is given by

$$\varphi_H = \tfrac{1}{2}\pi(h + k + l) \tag{2}$$

and f_H is the atomic scattering factor.

Under a uniaxial stress of magnitude σ applied parallel to the direction $l = [l_1, l_2, l_3]$ this becomes

$$|F_H|_\sigma^2 = 32f_H^2[1 + \cos(\varphi_H + \psi_H)] \tag{3}$$

where the stress-dependent change in phase is given by

$$\psi_H(\sigma, l) = 2\pi\bar{A}S_{44}\sigma(hl_2l_3 + kl_3l_1 + ll_1l_2). \tag{4}$$

S_{44} is a shear elastic constant and $\bar{A}$ is the internal strain parameter to be measured. The index H is omitted in all expressions below.

Reflections of the type $(0\ 0\ 4n + 2)$, where n is an integer, are strictly forbidden when the stress is zero:

$$|F_w|_0^2 = 0 \tag{5}$$

where w denotes weak. If we apply a compressive stress $|\sigma|$ parallel to the axis $l = (1/\sqrt{2})[1\bar{1}0]$, we have

$$\psi = (4n + 2)\pi\bar{A}S_{44}|\sigma|. \tag{6}$$

Under stress we find, using small angle approximations for $\sin \psi$ and $\cos \psi$, that

$$|F_w|_\sigma^2 = 16f^2\psi^2 \propto |\sigma|^2. \tag{7}$$

Reflections of the type $(0\ 0\ 4n)$ are strong because $\cos \varphi = 1$, and thus for zero stress

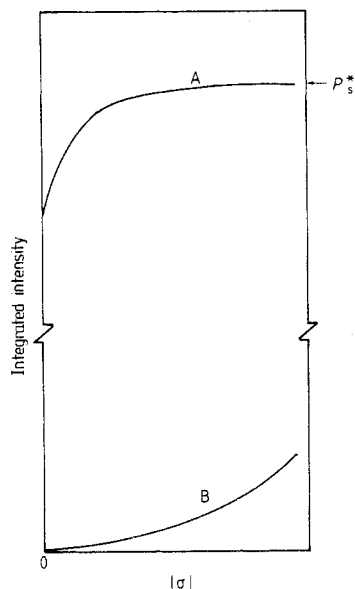$$|F_s|_0^2 = 64f^2 \tag{8}$$

where s denotes strong. Under stress

$$|F_s|_\sigma^2 = 64f^2(1 - \tfrac{1}{4}\psi^2) \tag{9}$$

which is effectively constant, since the final term is negligible.

To find $\bar{A}$ we need to measure the stress-dependence of two reflections, one weak and one strong. Their integrated intensities are given by

$$P_w = C_w|F_w|^2 \tag{10}$$

$$P_s = C_s|F_s|^2 \tag{11}$$

Figure 1. The variation of integrated intensity with stress: curve A, for a strong reflection; curve B, a weak reflection. The transition to the ideally imperfect state is shown in curve A and the asymptotic high-stress value P^*_s is indicated.
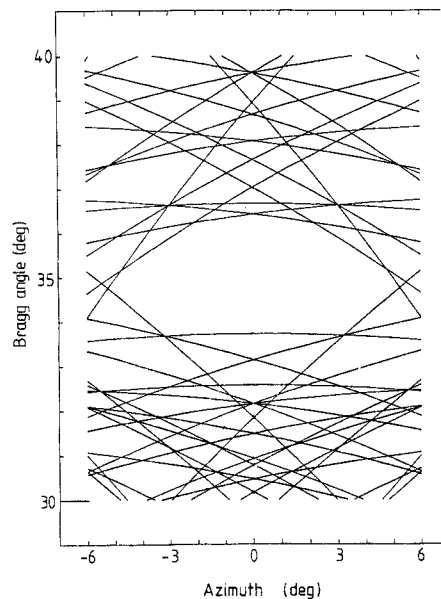
Figure 2. The loci of double reflections for the 006 reflection of diamond. The azimuth $\alpha = 0$ corresponds to the fiducial vector $[1\bar{1}0]$ perpendicular to the scattering plane. Along any curve there is an additional reflection in the Ewald sphere. Where n loci intersect there are $n - 1$ reflections simultaneously on the sphere. The open window around $(0°, 35°)$ is an ideal working point.

where the C_i depend on the Bragg angle, the beam polarisation and the energy of the diffracted photons. Figure 1 shows schematically the variation in P_i with stress for the two cases. P_w increases quadratically with stress, equation (7). P_s is independent of stress insofar as $|F_s|^2$ is concerned, but we must recall that equation (9) refers to an ideally imperfect crystal. If we start with a high quality crystal we expect P_s to have a lower value at low stresses but to approach the ideal value at stresses well below the largest stresses we apply to our crystals. If P^*_s is the high-stress limit then $|\bar{A}|$ is obtained from

$$|\bar{A}| = [2/(4n + 2)\pi S_{44}](C_s/C_w P^*_s)^{1/2} (f_s/f_w)\, d(P_w^{1/2})/\, d\,|\sigma|. \qquad (12)$$

The atomic scattering factors are corrected for temperature effects:

$$f_i = f_i^0 \exp(-M_i) \qquad (13)$$

where

$$M_i = B_i[(\sin\theta)/\lambda]^2 \qquad (14)$$

and the symbols have their usual meanings. The anomalous dispersion is exceedingly small as will be seen in § 3.

Table 1. Bulk property data for diamond. a is the lattice constant, S_{ij} the elastic constants and ρ the density.

a (Å)	S_{12} (TPa^{-1})	S_{44} (TPa^{-1})	ρ (g cm^{-3})
3.5670	−0.0991	1.7361	3.516

3. Experimental details

3.1. Sample

The sample is a type IIA diamond from D Drukker & Zn, Amsterdam. The sample has approximate dimensions $2 \times 1 \times 3$ mm^3, corresponding to the [001], [110] and [1$\bar{1}$0] directions. Bulk property data are given in table 1.

3.2. Uniaxial press

A frame of maraged steel holds a hydraulic cell and a pair of anvils. In the present experiment, special anvils of a hard sintered material (52% WC, 23% Ti, 15% Co, 10% Ta) were used. Zirconium shims were used to accommodate residual surface irregularity. The highest stress reached was 6.2 GPa (=62 kbar).

3.3. Working angle

Since the key measurement in this experiment is that of the integrated intensity of a weak reflection, it is important that it should not be contaminated by multiple reflection. It it thus necessary to choose a working (Bragg) angle within a clear window in the diagram showing the loci of multiple reflections. For convenience in setting up the crystal it is desirable to have the axis of zero azimuth (fiducial vector, chosen to be the [1$\bar{1}$0] direction and stress axis) parallel to the ω axis of the diffractometer. Thus the windows sought lie along $\alpha = 0$ in figure 2 which has been calculated in the way described by Cousins *et al* (1978). The same considerations apply to both reflection and transmission geometries. The clearest window appears between 34° and 36°. We have chosen to work at 34.4°.

3.4. X-ray configuration

The experiments were performed on the EDS (Energy Dispersive Scattering) Station at HASYLAB–DESY, Hamburg, in a configuration shown in figure 3 (see Olsen *et al* (1981, 1986) for details). The x-ray scattering is recorded in the horizontal plane. The electron storage ring operates at 5.3 GeV (high-energy physics run). The horizontally polarised beam is constrained to a 100×100 μm^2 cross section by horizontal and vertical slits and is then intercepted by a gold-coated mirror. Total reflection at a small glancing angle is used for eliminating the high-energy x-rays. After total reflection, the beam cross section is further reduced to 40×40 μm^2 by a pair of crossed slits. An ionisation chamber is used for monitoring the incident beam intensity. The diamond sample is adjusted for Bragg reflection in the (001) planes in symmetric transmission geometry. The vertical [1$\bar{1}$0] stress axis is perpendicular to the plane of the paper in figure 3. The
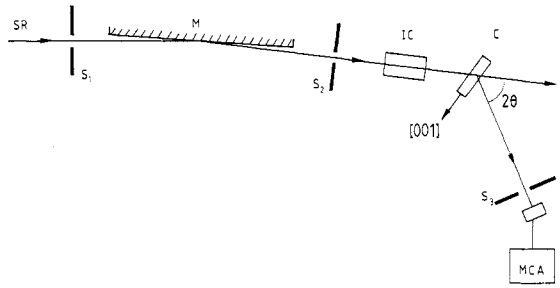
Figure 3. The layout used in the present experiments. Key: SR, synchrotron radiation from the storage ring; s_1, s_2 and s_3, slits; M, gold coated mirror; IC, ionisation chamber; C, diamond crystal reflecting in symmetrical transmission geometry; D, solid state detector; MCA, multi-channel analyser. The plane of the paper is the horizontal plane.

diffracted beam is detected by a solid-state detector connected through appropriate electronics to a multichannel pulse-height analyser consisting of the Canberra System 100 installed in an IBM PC-AT. The solid-state detector is made of high purity germanium and has an energy resolution of 145 eV (FWHM) at 5.9 keV.

3.5. The energy-dispersive mode

The fixed crystal will diffract in an energy-dispersive manner and integrated intensities will be given by

$$P_i = 2hcr_e^2 N^2 i_0(E_i)S_0 A_c |F_i|^2 d_i^2 \cos^2(2\theta) \tag{15}$$

(Buras and Gerward 1975) where h is Planck's constant, c the velocity of light, r_e the classical electron radius, N the number of unit cells per unit volume, $i_0(E)$ the incident intensity per unit energy range, S_0 the cross section of the incident beam and d_i the lattice plane spacing. In symmetrical transmission geometry the absorption correction A_c is given by

$$A_c = (t/\cos \theta) \exp(- \mu_m \rho t/\cos \theta) \tag{16}$$

where t is the thickness of the crystal, μ_m the mass attenuation coefficient and ρ the density. The lattice plane spacings d_i are related to the energy through the Bragg equation which is conveniently written

$$E_i d_i \sin \theta = \tfrac{1}{2}hc. \tag{17}$$

In the energy-dispersive mode, the weak and strong reflections are collected simultaneously for a fixed Bragg angle. The values of the energies and other relevant diffraction data are listed in table 2. Comparison of (15) with (10) or (11) allows the C_i to be inferred. Omitting constant factors one obtains

$$C_i = i_0(E_i)d_i^2 \exp[-\mu_m(E_i)\rho t/\cos \theta]. \tag{18}$$

3.6. Energy calibration

The conversion from channel number to energy is obtained by collecting $K\alpha$ and $K\beta$ fluorescence radiation from several elements. The known energies of these lines are

**Table 2.** Diamond data for Bragg reflections at $\theta = 34.4°$. Symbols are defined in the text.

Parameter	Diamond reflection		Parameter	Diamond reflection	
	006	008		006	008
E (keV)	18.4570	24.6094	$\Delta f'$	0.0046	0.0028
$(\sin\theta)/\lambda$ (Å^{-1})	0.84104	1.12139	$f'(\equiv f^0 + \Delta f')$	1.2834	0.9954
B (Å^2)	0.1445	0.1445	$f''(\equiv\Delta f'')$	0.0014	0.0007
$M\{\equiv B[(\sin\theta)/\lambda]^2\}$	0.1022	0.1817	$f(\equiv(f'^2 + f''^2)^{1/2})$	1.2834	0.9954
$T\ (\equiv\exp(-M))$	0.9028	0.8338	fT	1.1587	0.8300
f^0	1.2788	0.9926	μ_m (cm^2 g^{-1})	0.5139	0.3201
f^0T	1.15456	0.8277			
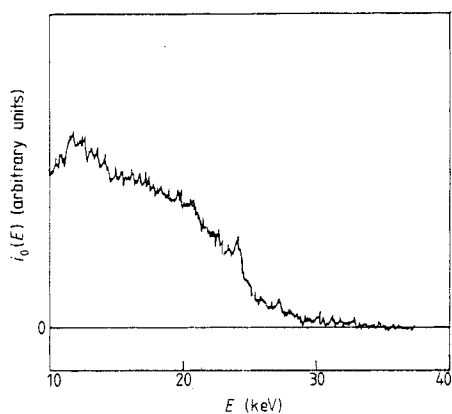
Figure 4. Spectral distribution of the incident beam (raw data). The function $i_0(E)$ is assumed to be a smooth curve through the data points. The small peak at 24 keV is In Kα excited inside the detector.
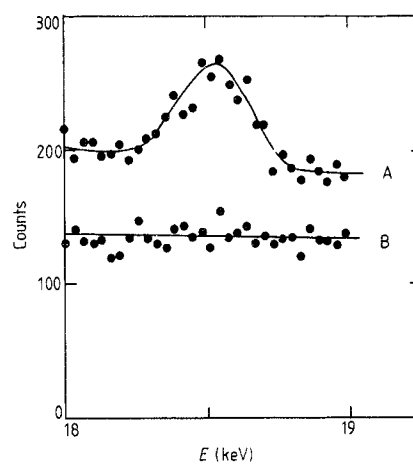
Figure 5. Samples of the MCA spectra showing the 006 reflection at 18.5 keV. Curve A, no stress; curve B, maximum stress (6.2 GPa).

fitted to a quadratic in the peak positions by the least squares method. A highly linear relation is expected, and is indeed found, together with a very small quadratic term.

3.7. Beam intensity calibration

The relative values of $i_0(E)$, the intensities as seen by the crystal, are needed before absolute values of $|\bar{A}|$ can be determined. This is a difficult exercise because the direct beam is very intense and solid-state detectors are very limited in the count rates that they can handle. Figure 4 shows the spectrum $i_0(E)$ obtained from scattering in the forward regime from a non-crystalline Kapton foil. The gold mirror was adjusted for a high-energy limit at about 30 keV. Thus of the strong 00l reflections, only the 004 and 008 were recorded, whereas the 0 0 12 and higher order reflections were excluded (cf energies given in table 2).
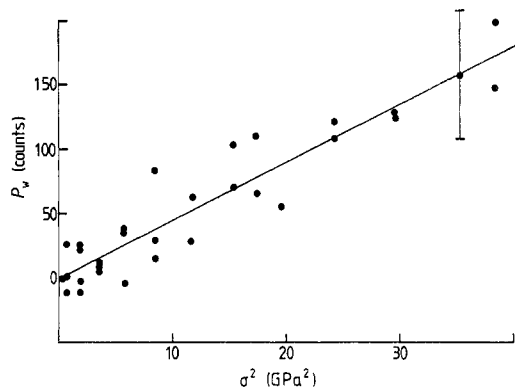
Figure 6. The variation of P_{006} with the square of the stress. The counting error is indicated at one point.
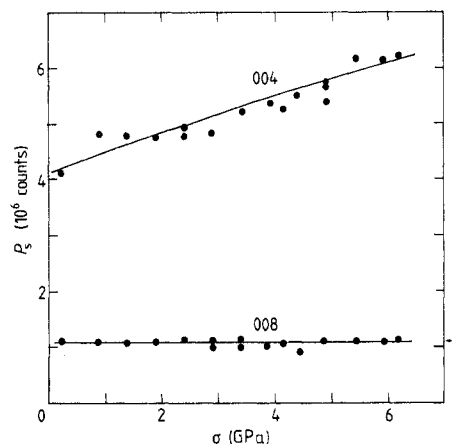
Figure 7. The variation P_s with stress: upper curve, P_{004}; lower curve, P_{008}.

4. Results

Figure 5 shows the 006 peak at the maximum stress 6.2 GPa. The variation of P_{006} with σ^2 is shown in figure 6. The stress dependences of the strong reflections are depicted in figure 7. It is seen that the 004 reflection does not reach the saturation value within the available pressure range, in contrast to the higher-order 008 reflection. The same observation has been made in the previous studies on silicon and germanium (Cousins *et al* 1982a,b).

After deducing P^*_{008} and using equation (12), the value of $|\bar{A}|$ shown below was found. Also listed is the more commonly quoted bond-bending parameter ζ, where $\zeta \equiv - 4\bar{A}$. It is known from stability considerations that $\bar{A}$ is negative, the mean values obtained from this experiment thus being

$$\bar{A} = - 0.031 \pm 0.005$$

and

$$\zeta = 0.125 \pm 0.020.$$

The large relative error is mainly due to the counting error in the very weak 006 reflection.

5. Concluding discussion

In table 3 are listed the theoretical values of the bond-bending parameter. All except that of Nielsen (1986) have been taken from table 1 of Cousins (1982) and the criterion for selection has been that the corresponding values for Si and Ge were in accord with our remeasured values (Cousins *et al* 1987). In passing down the table we are moving both chronologically and from the simplest parametrisations of lattice dynamics and elasticity to the computationally-intensive results of total energy calculations. The latter are very impressive over the whole range of cohesive energy, lattice parameter and elastic constant predictions.

Table 3. Values of the bond-bending parameter ζ of diamond.

Value	Source	Model
0.268	Musgrave (1963)	Simple valence-force-field
0.21	Keating (1966)	Nearest-neighbour non-central force constants
0.23	Lawætz (1973)	Via elastic constants and Raman frequency
0.12	Weber (1977)	Adiabatic bond-charge model
0.108	Nielsen (1986)	*Ab initio* pseudopotential calculation
0.125(20)	Present work	Experimental value

It is therefore gratifying to find that our experiments lead to a value that is at the lower end of the range of calculated values. The bond-bending parameter ζ varies with the external strain, and the theoretical values given in table 3 are valid in the limit of zero stress. Nielsen (1989) has calculated that for diamond and the stress geometry of the present experiment $\zeta = 0.114$ at 6.2 GPa. Thus ζ increases about 5% in the pressure range considered here.

Acknowledgments

References

Buras B and Gerward L 1975 *Acta Crystallogr.* A **31** 372–4
Cousins C S G, Gerward L and Olsen J S 1978 *Phys. Status Solidi* a **48** 113–9
Cousins C S G 1982 *J. Phys. C: Solid State Phys.* **15** 1857–72
Cousins C S G, Gerward L, Olsen J S, Selsmark B and Sheldon B J 1982a *J. Appl. Cryst.* **15** 154–9
Cousins C S G, Gerward L, Nielsen K, Olsen J S, Selsmark B, Sheldon B J and Webster G E 1982b *J. Phys. C: Solid State Phys.* **15** L651–4
Cousins C S G, Gerward L, Olsen J S, Selsmark B and Sheldon B J 1987 *J. Phys. C: Solid State Phys.* **20** 29–37
Keating P N 1966 *Phys. Rev.* **145** 637–45
Lawætz P 1973 *Phys. Status Solidi b* **57** 535–44
Musgrave M J P 1963 *Proc. R. Soc.* A **272** 503–28
Nielsen O H 1986 *Phys. Rev.* B **34** 5808–19
Nielsen O H 1989 private communication
Olsen J S, Buras B, Gerward L and Steenstrup S 1981 *J. Phys. E: Sci. Instrum.* **14** 1154–8
Olsen J S, Benedict U, Dabos S, Gerward L and Itié J-P 1986 *Physica* B **144** 56–60
Weber W 1977 *Phys. Rev.* B **15** 4789–803